



Effects of shifts in response preferences on characteristics of representation and real-time processing: An application to the Hering illusion

Michael J. Wenger¹ · James T. Townsend² · Lisa A. De Stefano¹ · Yanjun Liu²

Accepted: 20 October 2021 / Published online: 21 December 2021
© The Psychonomic Society, Inc. 2021

Abstract

The multidimensional generalization of signal detection theory known as General Recognition Theory (GRT, Ashby & Townsend, *Psychological Review*, 93, 154–179 1986) has been used to model and characterize the ways in which changes in encoded perceptual information and the application of decisional operators can produce patterns in behavior that are consistent with notions such as configural processing and representation. In particular, a set of studies (e.g., Cornes et al., 2011; Wenger & Ingvalson; 2002, 2003) have shown how decisional influences might exert themselves in situations of configural perception, such that effects such as the Thatcher illusion can be obtained by way of shifts in decisional criteria. The present investigation brought to bear the combined tools of GRT and Systems Factorial Technology (SFT, Little et al., 2017; Townsend & Nozawa, 1995) with a classical illusion, to show that it is possible to induce a shift in a decisional criterion by way of varying payoffs and that this shift is accompanied by regular changes in the workload capacity statistic. The combined sets of analyses on the same stimuli reveal orderly effects on the decisional criteria (i.e., the signal detection parameter c), report independence (suggesting perceptual independence), invariant measures of sensitivity (i.e., the signal detection parameter d'), and exhaustive parallel processing accompanied by super capacity. We therefore propose wider use of the combined sets of tools, further exploration of the ability of decisional alterations to affect processing times while leaving accuracy largely unscathed, and reaching out to explore more of the information processing mechanisms of classical illusions.

Keywords Decisional separability · General recognition theory · Systems factorial theory

Introduction

Scientific psychology got underway in the 19th century with a strong impetus from physics and physiology: think of Helmholtz, E.H. Weber, Fechner, and Wundt among others (see Boring, 1957). Murray and Link (2021) have recently shown that quantitative ideas were more frequent and deeply seated in the developing science than historians previously realized. A central accomplishment of the time was Fechner's psychophysics, which concerned the encoding of external energies into psychological values. Speaking broadly, if Fechner's psychophysics can be thought of as getting from the stimulus into the head (into psychological

representation via inner psychophysics; Boring, 1957; Dzharov & Colonius, 1999; Murray & Link, 2021), signal detection theory can be credited with getting back out of the head and into observable behavior (Ashby & Wenger, 2021; Link, 1994; Wixted, 2020). This foundational conceptualization is in part why William K. Estes, one of the giants of scientific psychology in the 20th century, considered signal detection theory to be “the most towering achievement of basic psychological research in the last half century” (Estes, 2002, p. 15).

A central distinction in signal detection theory is between the amount of perceptual or psychological evidence in favor of a response alternative and the predisposition to choose that alternative, regardless of the level of evidence in its favor. This distinction is typically quantified in classic signal detection theory in terms of sensitivity or discriminability (e.g., d') and response bias or response criterion (e.g., β or c , Ashby & Townsend, 1986; Ashby & Wenger, 2021; Macmillan & Creelman, 2004). Although there have been discussions of the necessity of the construct

✉ Michael J. Wenger
michael.j.wenger@ou.edu

¹ The University of Oklahoma, Norman, OK, USA

² Indiana University, Bloomington, IN, USA

of response bias (e.g., Balakrishnan, 1999), one of the strong empirical regularities in the application of signal detection theory has been the fact that response frequencies can quite easily be shifted using manipulations such as relative trial frequencies and payoffs (Egan, 1975; Macmillan & Creelman, 2004). In fact, this result has been found even at the level of features making up more complex stimulus patterns (Townsend et al., 1988).

The distinction between levels of perceptual evidence and the decisional criterion that is applied to that evidence was maintained in the multidimensional generalization of signal detection theory known as general recognition theory (GRT, Ashby & Townsend, 1986). Because of the introduction of more than a single perceptual dimension, the originators developed several key types of invariance (and their complements) across and among the distinct dimensions. Of course, as in single dimensional signal detection theory, concepts must still be embedded in a stochastic setting, but now that setting is multidimensional.

In GRT, the distinction is made among perceptual separability (PS), perceptual independence (PI), and decisional separability (DS). Perceptual separability signifies that changing the physical level of one dimension does not disturb the marginal probability distribution on the other dimensions. Perceptual independence is defined by the property that the joint probability distribution on values from the various dimensions be independent, expressed by that joint density function being expressed as the product of the separate marginal densities. Finally, decisional separability is interpreted as the decisional criterion on any one dimension being expressed by a single value, and thereby unaffected by values on the other dimensions. This constraint implies that the decision bounds in the ambient perceptual space be expressed as planes orthogonal to the pertinent dimension and parallel to the remainder of the (by definition, linear and mutually orthogonal) subspaces.

The majority of the published applications of GRT to date have used the simplest experimental paradigm: a 2×2 design in which two dimensions are manipulated at two levels each. Unfortunately, as convincingly documented by Silbert and Thomas (2013, 2017), there is an identifiability problem with respect to DS in this design: In any case in which DS is violated by a rotation of the linear decision bounds while satisfying PS, there always exists an alternative model that makes precisely the same empirical predictions and satisfies decisional separability while violating PS and with accompanying changes in the within-stimulus correlations, and these two models are related by a linear transformation.

This identifiability problem prompted Silbert and Thomas to suggest that applications of GRT that rely on the 2×2 design should be conducted under the a priori assumption that decisional separability holds (Silbert & Thomas, 2013, 2017). Acknowledging the inherent challenges with

the basic design, that approach obviates the use of one of the most valuable and long-standing assumptions of what Townsend and Ashby (1983, p. 465) called the *principle of correspondent change*. Specifically, if it is an empirical regularity that decisional criteria can be shifted, then the possibility of such a shift needs to be incorporated into the theory. This is what separates quantitative theory from curve fitting and assuming a priori that DS holds further seems to ignore the multitude of strong empirical regularities associated with classic manipulations such as variations in payoffs and stimulus frequency (Egan, 1975; Macmillan & Creelman, 2004; Townsend et al., 1988). And, when the possibility opens up that this linkage might be truly violated, there would be no avenue for its study. Thus, research has uncovered the important possibility that shifts in decisional operations may be contributors to effects that have previously been interpreted purely in terms of perceptual factors, such as is the case in the literatures on configural or holistic perception (e.g., Cornes et al., 2011; Wenger & Ingvalson, 2002; Wenger & Ingvalson, 2003). As a consequence, we sought to determine here whether, consistent with the logic of converging operations (Garner et al., 1956), there might be empirical regularities in independent measures associated with a *known* violation of DS.

In the present investigation, a classical illusion provides the terrain where several important goals may be pursued. The foremost goal is to further probe novel regions where bias manipulations might actually also perturb certain sensory functions. Toward this end, and following our recent work on perceptual learning (Wenger & Rhoten, 2020) we bring together within the same study GRT and systems factorial technology (SFT, Little et al., 2017; Townsend & Nozawa, 1995). GRT was invented primarily to investigate, as noted, dependencies among perceptual dimensions whereas SFT was designed primarily to identify mental architectures, decisional stopping rules, and workload capacity. Thus, one overriding aim was to perform experiments and allied analyses on the same individuals with the same or highly similar stimuli in such a way as to simultaneously shed light on each of the formerly isolated sets of mechanisms and properties. In so doing and beyond the proof of concept in joint application of SFT and GRT, we can thereby examine the effects of our bias manipulations on their conjoined findings.

Context: The Hering illusion

The specific experimental context for the present investigation is an illusion first described by Ewald Hering in the 19th century (Hering, 1861). The illusion is one in which one or more objectively vertical lines are perceived as being curved outward when superimposed on a background set of radial lines (see Fig. 1a). At least two physical factors appear

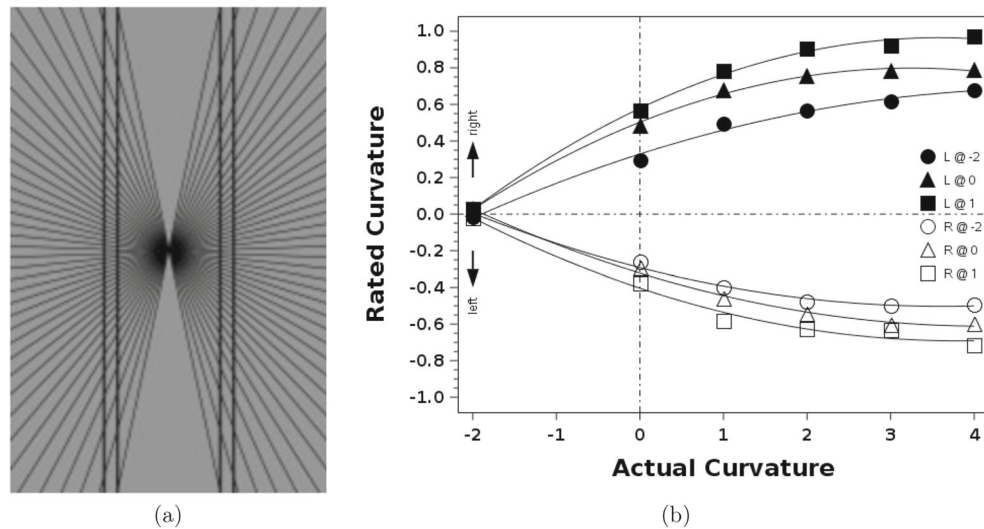


Fig. 1 **a** Example stimulus: in this example, the left and right *vertical lines* are objectively straight but are reliably judged to be curved outward. **b** A subset of the results from the rating experiment

to modulate the magnitude of the illusion: the number of radial lines and the physical congruence between the lines on either side of the center point (Hansen, 1961). The illusion offers a situation in which subjective perception does not correspond to the physical ground truth of the stimulus, which has distinct physical properties that allow for easy manipulation, and (by way of the influence of the congruence of the two sets of lines) offers a form of configularity. Thus, it gives us a chance to examine the potential function and effect of potential violations of DS in configural perception that are outside domains in which violations of DS as a source of configularity have been the source of some debate. In order to use the Hering illusion in this way, it was first necessary to determine the extent to which we could control the magnitude of perceived curvature as a function of the true level of curvature and the congruence between the left and right vertical lines in the stimuli. This was the purpose of Experiment 1.

In that preliminary experiment, we document the extent to which varying the objective curvature of the horizontal lines—from curved slightly inward to curved outward—affected the perceived curvature of each set of lines. Documenting the magnitude of the effect of actual curvature on perceived curvature allowed us to select the levels of curvature that we used in Experiment 2. In that second experiment, we varied payoffs either in favor of a curved response or in favor of a straight response in two tasks: a complete identification (CID) paradigm and a double factorial paradigm (DFP). The CID allowed us to examine performance from the perspective of GRT (Ashby & Townsend, 1986; Ashby & Wenger, 2021) in order to determine whether our payoff manipulation was successful

in inducing violations of DS. The DFP allowed us to examine performance from the perspective of SFT (Little et al., 2017; Townsend & Nozawa, 1995) in order to determine if violations of DS were regularly accompanied by any changes in processing architecture, stopping rule, independence in processing rates, or capacity.

Experiment 1

The intent of Experiment 1 was to quantify the extent to which the magnitude of the Hering illusion can be affected by factorially manipulating the level of curvature present in each set of vertical lines, holding the number of radial inducing lines constant. This was done by having participants rate the perceived curvature of the left and right set of lines separately, while varying the level of actual curvature in each set of lines.

Methods

Design

This experiment was designed as a 6 (level of left curvature: -2, 0 to +4 pixels) \times 6 (level of right curvature: -2, 0 to +4 pixels) \times 2 (set of lines to be judged: left, right) factorial, with all factors manipulated within participants. With respect to curvature, the units were the amount in pixels by which the vertical lines were curved either inward (negative values) or outward (positive values) at their maximum point of curvature. A value of 0 pixels curvature identifies vertical lines that were objectively straight. The

stimulus at -2 pixels was chosen on the basis of pilot work indicating that this level of inward curvature was reliably perceived to be straight.

Participants

A total of 25 participants (13 female) were recruited from the University of Oklahoma community and were compensated for their participation with a \$25 gift card.

Materials

An example stimulus is presented in Fig. 1a. Stimuli were constructed of black lines on a mid-scale gray background. At a constrained viewing distance of 79 cm, the stimuli subtended 2.6° and 3.9° of visual angle, horizontally and vertically. The pair of vertical lines subtended 1.3° of visual angle, horizontally. Stimuli were presented on a 53 cm (diagonal) grayscale CRT with a refresh rate of 100 Hz. Stimulus displays and response collection were controlled by DMDX (Forster & Forster, 2003). Stimulus onsets were synchronized to the vertical refresh rate of the monitor and all responses were timed to ± 1 ms.

Procedure

The experiment was performed in a dimly lit room, and participants adapted to the dim lighting for five min before beginning the experiment. The entire experiment was completed in approximately 45 min. The session began with the experimenter explaining the procedure for making the ratings and included four example trials, two in which the participant rated the perceived curvature of the left set of lines and two in which the participant rated the perceived curvature of the right set of lines.

Each trial in the experiment was self-initiated, and participants could take short breaks at any point. Order of the side to be rated (left, right) was randomly determined for each participant. Each trial began with a centrally presented black dot signaling that the trial was ready to begin. Participants initiated the trial by pressing the space bar on the computer keyboard. A fixation cross was then presented for a duration determined by sampling from an exponential distribution with a mean of 1100 ms, censored at 700 and 1500 ms. This was replaced by a pattern pre-mask, followed by the stimulus to be rated, followed by a pattern post-mask, each for 100 ms. This was followed by a linear response scale presented in the bottom half of the screen, whose midpoint was labeled “straight” and whose left and right end-points were labeled as “curved left” and “curved right”, respectively. Participants made their curvature ratings by clicking a point on this line, and no feedback was provided. Curvature ratings were normalized

to a range of -1 to 1 for each observer prior to analyses. Each level of curvature was rated ten times.

Results

The normalized curvature ratings were analyzed using two 6 (level of left curvature) \times 6 (level of right curvature) repeated-measures analyses of variance (ANOVAs), one each for the ratings of the left and right sides. Results are presented in Table 1, and a subset of the ratings are plotted in Fig. 1b. The normalized responses were remarkably consistent across participants. For both the left and right sides, the main effects of curvature on each side were reliable, indicating that perceived curvature increased with actual curvature. In addition, the interaction of the two sides was reliable, indicating that the perceived curvature of the side being rated was affected by the curvature of the other side, with the interaction being to increase perceived curvature of one side if the other side was more curved. All levels of actual curvature, including curvature of 0 (objectively straight) but excluding curvature of -2 (curved inward) resulted in curvature ratings that were reliably different from 0. Ratings at curvature of -2 were all not reliably different from 0. This is the Hering illusion: lines that were objectively curved inward were reliably judged to be straight while lines that were objectively straight were reliably judged to be curved outward. Levels of curvature beyond +1 did not reliably differ from one another on either side. Consequently, for clarity of presentation, we restrict the data in Fig. 1b to levels -2, 0, and +1 on both sides.

Discussion

The results of Experiment 1 affirm that the presence and magnitude of the Hering illusion can be affected by the congruence of curvature between the two sets of lines. This is important as Experiment 2 requires that we be able to manipulate the magnitude of the illusion. In addition, this

Table 1 Results of the repeated-measures ANOVAs on the curvature ratings

Side	Judged	Factor	<i>df</i>	<i>MSE</i>	<i>F</i>
Left		Left (L)	5	0.009	217.84 [‡]
		Right (R)	5	0.007	159.76 [‡]
		L \times R	25	0.008	10.01 [‡]
Right		Right (R)	5	0.008	275.72 [‡]
		Left (L)	5	0.010	232.10 [‡]
		R \times L	25	0.007	14.04 [‡]

Note: [‡] = $p < .001$

suggests a potential type of configularity that we wish to characterize in terms of independence vs. dependence in the encoded information and the forms of processing that are applied to that information.

Experiment 2

In Experiment 2, we sought to use the combined tools of GRT and SFT to determine whether an induced violation of DS (in the complete identification task, CID) would be accompanied by regular changes in characteristics of processing in the double factorial paradigm (DFP). Participants performed both tasks twice, once in a neutral payoff condition and then in one of the two biased conditions. Half of the participants were transferred to a condition which preferentially rewarded responses indicating perceived curvature and half were transferred to a condition which preferentially rewarded responses indicating an absence of perceived curvature.

Methods

Design

The CID was designed as a 2 (subjective curvature on the left: absent, present) × 2 (subjective curvature on the right: absent, present) × 2 (payoffs: neutral, biased) complete factorial, with all factors manipulated within participants. The neutral payoff condition was always performed first, and half of the participants were transferred to one of the two bias conditions. The payoff matrices for the three bias conditions in the CID are presented in Table 2.

The DFP was designed as a nested pair of 2 × 2 factorial designs. The outer factorial was a 2 (subjective curvature on the left: absent, present) × 2 (subjective curvature on the right: absent, present) factorial. The inner factorial pertained to the stimuli in which subjective curvature was present

on both sides and was a 2 (ambiguity of the curvature on the left: ambiguous, unambiguous) × 2 (ambiguity of the curvature on the right: ambiguous, unambiguous) factorial, with ambiguity manipulated by way of the actual amount of curvature. All factors were manipulated within participants. As with the CID, the neutral bias condition was performed first, then half of the participants were transferred to a condition biased in favor of curvature and half were transferred to a condition biased against curvature. The payoff matrices for the three bias conditions of the DFP are presented in Table 3.

Participants

Eight participants (five female) were recruited from the university community and were compensated with a \$150 gift card. Data from one participant could not be used due to the participant withdrawing from the experiment before completion.

Materials

Stimuli were selected from those rated during experiment 1. Example stimuli for both tasks are presented in Figure 2. The stimulus with lines curved in by two pixels was considered subjectively straight, while the stimulus with 0 pixels of curvature was considered ambiguously curved, and the stimulus with 1 pixel of outward curvature was considered unambiguously curved. Participants viewed the images from a constrained distance of 79 cm, with the images overall subtending 2.6° and 3.9° of visual angle, horizontally and vertically, and the pair of vertical lines subtending 1.3° of visual angle horizontally. Stimuli were presented on a 53 cm (diagonal) grayscale CRT with a refresh rate of 100 Hz. Stimuli were displayed and responses were collected using DMDX (Forster & Forster, 2003). Stimulus onsets were synchronized to the vertical refresh rate of the monitor. All responses were timed to +/- 1 ms.

Table 2 Payoff matrices for the CID as a function of the biasing conditions

Stimulus	Responses				Prefer Curvature				Prefer Straight			
	Neutral	Left	Right	Both	Neither	Left	Right	Both	Neither	Left	Right	Both
Neither	5	0	0	-5	3	0	0	0	3	-2	-2	-2
Left	0	5	-5	0	-4	3	0	0	2	3	-2	-2
Right	0	-5	5	0	-4	0	3	0	2	-2	3	-2
Both	-5	0	0	5	-4	0	0	3	-2	-2	-2	3

Note: Stimuli and responses are labeled according to the perceived outward curvature in the left and right set of lines

Table 3 Payoff matrixes for the DFP

Left lines	Right lines and bias condition		Prefer Curved		Prefer Straight	
	Neutral Curved	Straight	Curved	Straight	Curved	Straight
Curved	5	−5	5	−5	1	−1
Straight	−5	5	1	1	−5	5

Payoffs here refer to the payoffs received for a correct response in the DFP in the conditions defined by the subjective curvature of the left and right set of lines

Procedure

Participants completed 16 sessions lasting approximately 1 h each. They were offered three 5-min breaks during each session. Each session was completed in darkness and participants were adapted to the dark for 5 min before every session and after each break. Figure 3 summarizes the procedure for Experiment 2.

Participants were randomly assigned to begin with either three sessions of the CID or five sessions of the DFP before moving on to complete the other task. The first eight sessions always had neutral payoffs. After both paradigms were completed, participants engaged in them again in the same order, this time with the appropriately biased payoffs.

During both the CID and DFP, participants accumulated points for their selections on the basis of the payoffs. The points were constantly shown in the bottom right of the screen and reset after each block. At the start of every block, participants were reminded of their previous block score (or, in the case of the first block of the day, their previous day's final block score) and encouraged to do their best

to beat their score. At the end of each block of trials, the participant's block score was compared to their previous block. If the participant beat their previous score, they could select a piece of candy from a dish.

Complete identification paradigm Participants completed two series of three CID sessions, each consisting of four blocks of 192 trials, for a total of 768 trials per session. Each of four stimuli appeared 48 times per block. During the first session of each series, participants were instructed to press one of four keys on the number pad to identify which stimulus they saw, and they were given 12 practice trials.

Each trial began with a fixation point in the center of the screen that signaled to the participant that the trial could begin. Participants pressed the space bar to begin the trial. A fixation cross was presented for a duration determined by sampling from an exponential distribution with a mean of 1000 ms, censored at 500 and 1500 ms. This was followed by a pattern pre-mask, the stimulus, and a pattern post-mask, each for 100 ms. Responses were collected, and participants heard an 800-Hz tone if their judgment of both sides was

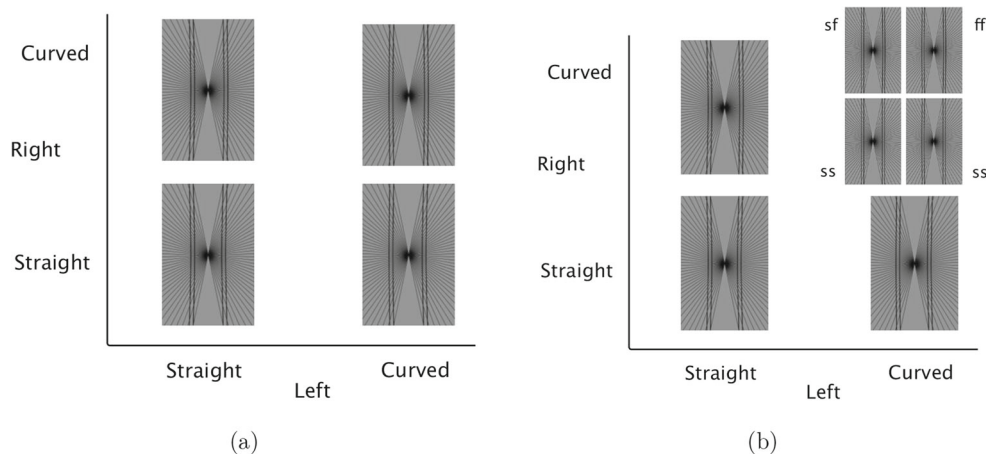


Fig. 2 **a** Example stimuli for the CID. **b** Example stimuli for the DFP, including the four stimuli in the inner (nested) factorial, manipulated for selective influence on the processing times of the left and right set of lines. Note: s = slow, f = fast

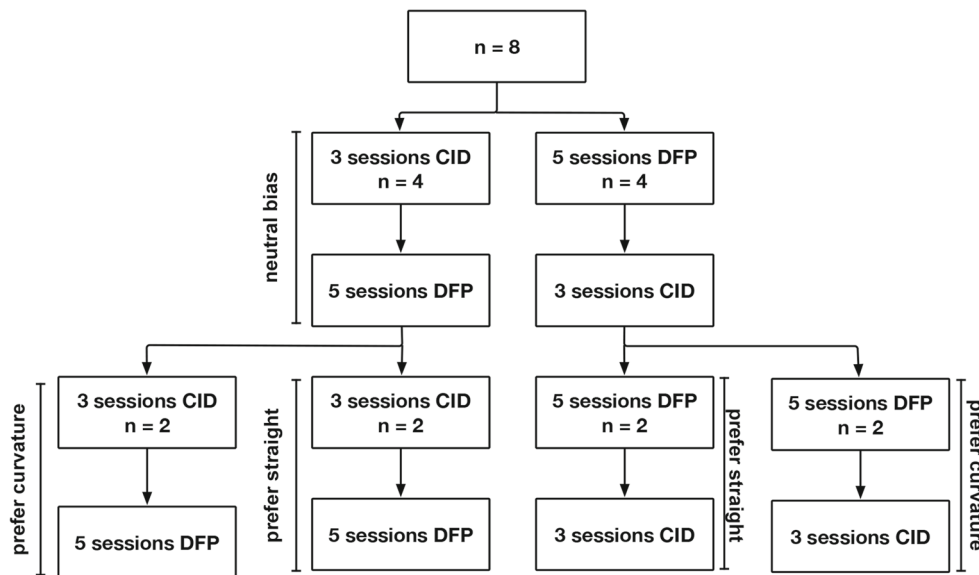


Fig. 3 a Overview of the procedure used in experiment 2

correct, a 660-Hz tone if their judgment was only correct about one side, and a 440-Hz tone if they were incorrect about both sides.

Double factorial paradigm Participants completed two series of five DFP sessions, each consisting of four blocks of 192 trials, for a total of 768 trials per session. In each block, half of the presented stimuli appeared subjectively straight on both sides. Of the other half, 64 appeared straight on one side while the other side was unambiguously curved; 16 appeared unambiguously curved on one side and ambiguously curved on the other; eight appeared ambiguously curved on both sides; and eight appeared unambiguously curved on both sides. Participants were instructed to press a key assigned to their dominant hand if either set of lines were perceived to be curved, and a key assigned to their non-dominant hand if neither set of lines was perceived to be curved. Participants began each session with four practice trials.

Each trial began with a fixation point in the center of the screen that signaled to the participant that the trial could begin. Participants pressed the space bar to begin the trial. A fixation cross was presented for a duration determined by sampling from an exponential distribution with a mean of 1000 ms, censored at 500 and 1500 ms. This was followed by a pattern pre-mask, the stimulus, and a pattern post-mask, each for 100 ms. Responses were collected and participants were presented with an 800-Hz tone if their judgment was correct and a 440-Hz tone if their response was incorrect.

Results

Complete identification task

We first examined the data for any violations of marginal response invariance (MRI) and timed marginal response invariance (tMRI, Townsend et al., 2012), given the critical and non-parametric role that MRI and tMRI play in drawing inferences concerning DS and PS (Silbert & Thomas, 2013; 2017).¹ MRI holds for the *i*th level of the left side if

$$\begin{aligned}
 p(l_i|L_i R_s) &= p(l_i r_s|L_i R_s) + p(l_i r_c|L_i R_s) \\
 &= p(l_i r_s|L_i R_c) + p(l_i r_c|L_i R_c) \\
 &= p(l_i|L_i R_c)
 \end{aligned}$$

where L and R indicate the left and right set of lines, respectively, and the subscripts s and c indicate straight and curved. tMRI holds for the *i*th level of the left side if, for all $t > 0$

$$\begin{aligned}
 p(l_i, T \leq t|L_i R_s) &= p(l_i r_s, T \leq t|L_i R_s) + p(l_i r_c, T \leq t|L_i R_s) \\
 &= p(l_i r_s, T \leq t|L_i R_c) + p(l_i r_c, T \leq t|L_i R_c) \\
 &= p(l_i, T \leq t|L_i R_c)
 \end{aligned}$$

The results of these comparisons are presented in Tables 4 and 5. No violations of MRI or tMRI were obtained for any

¹Readers interested in the details of each of the measures assessed in the CID and DFP should consult relevant primary sources (including Ashby & Townsend, 1986; Silbert & Hawkins, 2016; Townsend & Nozawa, 1995; Townsend et al., 2012).

Table 4 Tests of marginal response invariance

Obs	Neutral Comparison	Neutral			Prefer Curvature		
		<i>p</i> 1	<i>p</i> 2	<i>z</i>	<i>p</i> 1	<i>p</i> 2	<i>z</i>
1	L, straight	0.778	0.793	0.253	0.737	0.711	0.885
	L, curved	0.767	0.752	0.235	0.807	0.843	1.475 ⁺
	R, straight	0.789	0.802	0.260	0.785	0.785	0.000
	R, curved	0.759	0.774	0.239	0.757	0.817	2.255*
4	L, straight	0.785	0.785	0.245	0.761	0.752	0.307
	L, curved	0.724	0.724	0.211	0.796	0.813	0.665
	R, straight	0.685	0.685	0.204	0.724	0.722	0.074
	R, curved	0.743	0.743	0.226	0.843	0.922	3.687 [‡]
6	L, straight	0.859	0.824	0.304	0.863	0.822	1.719*
	L, curved	0.859	0.843	0.315	0.843	0.817	1.054
	R, straight	0.730	0.748	0.222	0.800	0.752	1.740*
	R, curved	0.820	0.859	0.255	0.763	0.943	7.733 [‡]
8	L, straight	0.741	0.715	0.216	0.833	0.815	0.692
	L, curved	0.798	0.820	0.271	0.867	0.854	0.572
	R, straight	0.863	0.848	0.321	0.861	0.817	1.795*
	R, curved	0.846	0.800	0.284	0.878	0.913	1.725*
2	Neutral				Prefer Straight		
	L, straight	0.830	0.804	0.279	0.783	0.787	0.160
	L, curved	0.796	0.787	0.257	0.824	0.817	0.258
	R, straight	0.804	0.780	0.258	0.878	0.791	3.551 [‡]
7	R, curved	0.848	0.813	0.292	0.746	0.822	2.803 [†]
	L, straight	0.863	0.841	0.317	0.874	0.854	0.866
	L, curved	0.857	0.822	0.301	0.783	0.830	1.836*
	R, straight	0.839	0.839	0.000	0.857	0.826	1.263
10	R, curved	0.809	0.774	0.257	0.807	0.817	0.422
	L, straight	0.848	0.848	0.311	0.933	0.907	1.455 ⁺
	L, curved	0.861	0.885	0.345	0.846	0.898	2.366 [†]
	R, straight	0.870	0.887	0.354	0.867	0.889	1.008
	R, curved	0.857	0.870	0.331	0.909	0.922	0.710

Note: L = left set of lines, R = right set of lines. ⁺ = 0.05 ≤ *p* < 0.10, * = *p* < .05, [†] = *p* < .01, [‡] = *p* < .001

of the observers in the neutral payoff condition. A total of seven violations of MRI were obtained in the condition in which curvature was preferred, and a total of five violations of MRI were obtained in the condition in which a straight response was preferred. In each case, the inequalities in the response proportions were consistent with the intended bias in favor of either the curved/curved or straight/straight stimulus. That is, the failures of MRI in the condition in which curvature was preferred showed either an increase in the proportion of responses indicating curvature or a decrease in the proportion of responses indicating a lack of curvature. The opposite was true for the condition in which a straight response was preferred. In this case, the failures of MRI were either an increase in the proportion of straight responses or a decrease in the proportion of straight responses. A total of five violations of tMRI were obtained

in the condition in which the bias was in favor of curvature, and in all five cases the violation occurred when the second dimension was curved. A total of seven violations of tMRI were obtained in the condition in which bias favored a straight response, and four of those seven cases occurred when the second dimension was straight. Thus, the MRI and tMRI results suggest potential violations of either PS or DS, but only in the biased conditions.

We next considered comparisons involving the marginal signal detection measures of discriminability (*d'*) and bias (*c*), calculated according to the standard equal-variance gaussian model. These comparisons took the form

$$d'(L, R_s) = d'(L, R_c)$$

$$c(L, R_s) = c(L, R_c)$$

Table 5 Tests of timed marginal response invariance

Obs	Comparison	Neutral	Prefer curvature	Obs	Comparison	Neutral	Prefer straight
		<i>D</i>	<i>D</i>			<i>D</i>	<i>D</i>
1	L, R straight	0.036	0.078	2	L, R straight	0.045	0.093
	L, R curved	0.035	0.039		L, R curved	0.030	0.113*
	R, L straight	0.033	0.086		R, L straight	0.029	0.108*
	R, L curved	0.022	0.135 [†]		R, L curved	0.035	0.077
4	L, R straight	0.027	0.054	7	L, R straight	0.024	0.112*
	L, R curved	0.022	0.230 [‡]		L, R curved	0.030	0.128 [†]
	R, L straight	0.023	0.061		R, L straight	0.038	0.170 [‡]
	R, L curved	0.019	0.137 [†]		R, L curved	0.019	0.066
6	L, R straight	0.031	0.050	10	L, R straight	0.017	0.095*
	L, R curved	0.033	0.254 [‡]		L, R curved	0.024	0.104*
	R, L straight	0.036	0.028		R, L straight	0.017	0.055
	R, L curved	0.021	0.210 [‡]		R, L curved	0.023	0.041
8	L, R straight	0.028	0.048				
	L, R curved	0.021	0.077				
	R, L straight	0.027	0.050				
	R, L curved	0.028	0.035				

Note: L = left set of lines, R = right set of lines. ⁺ = 0.05 ≤ *p* < 0.10, * = *p* < .05, [†] = *p* < .01, [‡] = *p* < .001

These are presented for the neutral condition and the condition biased in favor of curvature in Table 6 and for the neutral condition and the condition biased against curvature in Table 7. Equality of the parameters was assessed using

95% confidence intervals (Gourevitch & Galanter, 1967). No reliable differences for either marginal measure were obtained in the neutral conditions. We found one reliable inequality for *d'*, for observer 6 in the condition favoring

Table 6 Marginal signal detection parameters for the four observers who were switched to a bias in favor of curvature

Obs	Neutral				Prefer curvature				
	Comparison	Hit rate	FA rate	<i>d'</i>	<i>c</i>	Hit rate	FA rate	<i>d'</i>	<i>c</i>
1	L with R straight	0.767	0.222	1.058	0.013	0.767	0.261	0.969	-0.032
	L with R curved	0.752	0.207	1.061	0.049	0.852	0.267	1.178	-0.150
	R with L straight	0.759	0.211	1.065	0.036	0.763	0.215	1.064	0.026
	R with L curved	0.774	0.198	1.132	0.035	0.778	0.222	1.084	0.000
4	L with R straight	0.724	0.215	0.978	0.069	0.783	0.222	1.094	-0.005
	L with R curved	0.713	0.235	0.909	0.057	0.789	0.263	1.016	-0.060
	R with L straight	0.743	0.315	0.803	-0.061	0.846	0.309	1.073	-0.183
	R with L curved	0.748	0.274	0.897	-0.024	0.887	0.315	1.196	-0.258
6	L with R straight	0.859	0.141	1.520	0.000	0.830	0.163	1.370	0.009
	L with R curved	0.843	0.176	1.371	-0.028	0.850	0.165	1.421	-0.022
	R with L straight	0.820	0.270	1.080	-0.106	0.772	0.230	1.048	-0.003
	R with L curved	0.759	0.252	0.969	-0.012	0.943	0.272	1.550	-0.345
8	L with R straight	0.798	0.257	1.052	-0.064	0.852	0.172	1.409	-0.035
	L with R curved	0.820	0.285	1.048	-0.122	0.880	0.187	1.461	-0.102
	R with L straight	0.846	0.135	1.500	0.030	0.900	0.148	1.646	-0.083
	R with L curved	0.800	0.152	1.321	0.066	0.917	0.222	1.523	-0.220

Grayed squares indicate values that were reliably different from one another based on estimated confidence intervals. Note: L = left set of lines, R = right set of lines

Table 7 Marginal signal detection parameters for the four observers who were switched to a bias against curvature

Obs	Neutral				Prefer straight				
	Comparison	Hit rate	FA rate	d'	c	Hit rate	FA rate	d'	c
2	L with R straight	0.796	0.170	1.260	0.046	0.826	0.154	1.384	0.028
	L with R curved	0.787	0.196	1.169	0.022	0.828	0.165	1.358	0.009
	R with L straight	0.848	0.196	1.332	-0.060	0.750	0.146	1.223	0.135
	R with L curved	0.813	0.220	1.176	-0.041	0.828	0.187	1.299	-0.021
7	L with R straight	0.857	0.137	1.527	0.050	0.754	0.096	1.411	0.219
	L with R curved	0.822	0.159	1.359	0.048	0.854	0.154	1.466	-0.013
	R with L straight	0.809	0.161	1.318	0.048	0.809	0.126	1.427	0.096
	R with L curved	0.774	0.161	1.232	0.047	0.850	0.161	1.434	-0.016
10	L with R straight	0.861	0.152	1.493	-0.020	0.857	0.096	1.677	0.086
	L with R curved	0.885	0.152	1.574	-0.061	0.883	0.122	1.665	-0.008
	R with L straight	0.857	0.130	1.548	0.021	0.885	0.111	1.712	0.008
	R with L curved	0.870	0.113	1.651	0.030	0.907	0.128	1.735	-0.007

Grayed squares indicate values that were reliably different from one another based on estimated confidence intervals. Note: L = left set of lines, R = right set of lines

curvature. In addition, we obtained reliable inequalities for c on one dimension for all observers in both biasing conditions, with the direction of the shifts in the value of c being consistent with the biasing manipulation. That is, marginal c became more negative (liberal) in the condition favoring curvature and became more positive (conservative) in the condition favoring a lack of curvature. This suggests that our manipulation was able to induce the desired violations of decisional separability in a regular and

interpretable way, although this was true for only one of the dimensions.

We then examined the data for any violations of report independence (RI) and timed report independence (tRI, Townsend et al., 2012). RI holds for stimulus $L_i R_j$ if

$$p(l_i r_j | L_i R_j) = [p(l_i r_s | L_i R_j) + p(l_i r_c | L_i R_j)] \times [p(l_s r_j | L_i R_j) + p(l_c r_j | L_i R_j)]$$

Table 8 Tests of report independence

Obs	Stimulus	χ^2		Obs	Stimulus	χ^2	
		Neutral	Prefer curvature			Neutral	Prefer straight
1	Straight/Straight	0.018	1.163	2	Straight/Straight	0.501	0.792
	Straight/Curved	1.116	0.318		Straight/Curved	0.778	0.419
	Curved/Straight	0.053	0.374		Curved/Straight	0.481	0.847
	Curved/Curved	0.673	0.507		Curved/Curved	1.154	0.371
4	Straight/Straight	1.616	0.729	7	Straight/Straight	0.175	0.718
	Straight/Curved	0.031	0.768		Straight/Curved	0.436	0.665
	Curved/Straight	0.034	0.805		Curved/Straight	0.794	0.330
	Curved/Curved	1.035	0.636		Curved/Curved	0.529	0.618
6	Straight/Straight	0.567	0.265	10	Straight/Straight	0.190	0.331
	Straight/Curved	0.172	0.831		Straight/Curved	0.001	0.199
	Curved/Straight	0.320	0.039		Curved/Straight	0.010	0.154
	Curved/Curved	0.371	0.410		Curved/Curved	0.189	0.001
8	Straight/Straight	0.610	0.401				
	Straight/Curved	0.259	0.407				
	Curved/Straight	0.075	0.510				
	Curved/Curved	0.015	0.256				

Table 9 Tests of timed report independence

Obs	Stimulus	<i>D</i>		Obs	Stimulus	<i>D</i>	
		Neutral	Prefer curvature			Neutral	Prefer straight
1	Straight/Straight	0.002	0.002	2	Straight/Straight	0.005	0.007
	Straight/Curved	0.002	0.005		Straight/Curved	0.005	0.003
	Curved/Straight	0.003	0.004		Curved/Straight	0.009	0.005
	Curved/Curved	0.004	0.007		Curved/Curved	0.002	0.011
4	Straight/Straight	0.004	0.015	7	Straight/Straight	0.001	0.001
	Straight/Curved	0.011	0.009		Straight/Curved	0.001	0.002
	Curved/Straight	0.004	0.008		Curved/Straight	0.001	0.001
	Curved/Curved	0.006	0.005		Curved/Curved	0.001	0.001
6	Straight/Straight	0.001	0.002	10	Straight/Straight	0.001	0.001
	Straight/Curved	0.003	0.001		Straight/Curved	0.002	0.001
	Curved/Straight	0.001	0.001		Curved/Straight	0.002	0.002
	Curved/Curved	0.001	0.001		Curved/Curved	0.001	0.001
8	Straight/Straight	0.001	0.003				
	Straight/Curved	0.001	0.001				
	Curved/Straight	0.002	0.003				
	Curved/Curved	0.001	0.002				

tRI holds for stimulus $L_i R_j$ if

$$\begin{aligned}
 p(RT(i, j) \leq t | L_i R_j) &\times p(RT(\cdot, \cdot) \\
 &\leq t | L_i R_j) = p(RT(i, \cdot) \leq t | L_i, R_j) \\
 &\times p(RT(\cdot, j) \leq t | L_i R_j)
 \end{aligned}$$

Results for the checks on RI are presented in Table 8 and the results for tRI are presented in Table 9. No violations of RI or tRI were obtained for any of the observers in either of the

biasing conditions, suggesting that there were no violations of PI in either the neutral or either one of the bias conditions.

To this point, the data suggest no violations of PI in either the neutral or either biased condition, and only a single violation of PS for one observer in the positive bias condition. In contrast, while there were no violations of DS in the neutral conditions, every observer in the biased conditions showed potential violations of DS, in directions consistent with the biasing manipulation.

Table 10 Best-fitting models for each of the observers in each of the bias conditions

Obs	Bias	PI	PS	DS	Parameters	ln(L)	AIC
1	neutral	T	T	T	4	-1951.120	3910.240
	prefer curvature	T	T	F(L)	5	-1946.612	3903.223
4	neutral	T	T	T	4	-2173.572	4355.144
	prefer curvature	T	T	F(R)	5	-1915.845	3847.690
6	neutral	T	T	T	4	-1825.296	3658.592
	prefer curvature	T	F(R)	F(R)	6	-1674.980	3361.961
8	neutral	T	T	T	4	-1793.827	3595.654
	prefer curvature	T	T	F(R)	5	-1505.011	3020.021
2	neutral	T	T	T	4	-1797.235	3602.471
	prefer straight	T	T	F(R)	5	-1703.313	3416.626
7	neutral	T	T	T	4	-1668.292	3344.584
	prefer straight	T	T	F(L)	5	-1581.755	3173.510
10	neutral	T	T	T	4	-1451.309	2910.078
	prefer straight	T	T	F(L)	5	-1312.756	2635.511

Note: L = left set of lines, R = right set of lines, T = property was true (no violation), F = property failed (violation), AIC = Akaike information criterion, PI = perceptual independence, PS = perceptual separability, DS = decisional separability

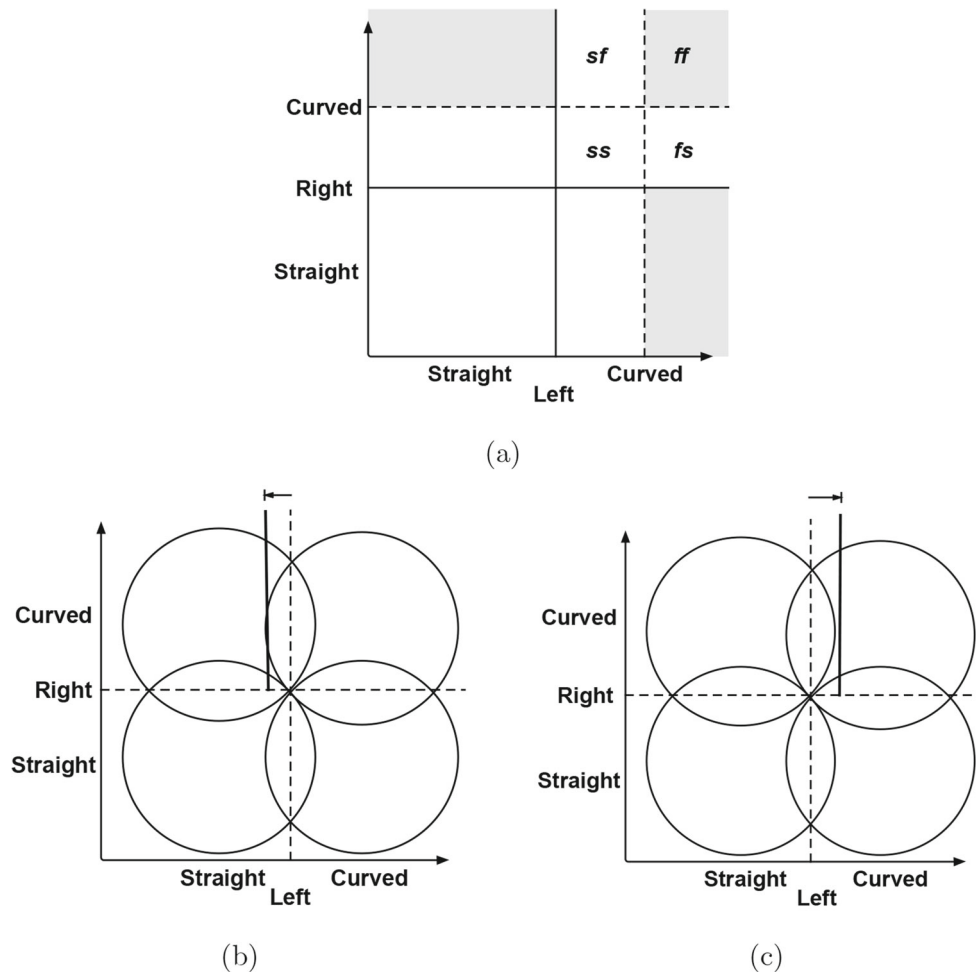


Fig. 4 Effects of a violation of DS on capacity: **a** Correspondence between the cells in the CID that are used to infer a violation of DS (*shaded*) and the cells in the DFP that are used to estimate capacity. **b** The shift in the decision bound in favor of a curved response in the curved/curved trials. **(c)** The shift in the decision bound in favor of a straight response in the curved/curved trials

However, given the known weaknesses of the 2×2 design, we checked these inferences using a hierarchy of constrained multivariate Gaussian models (Thomas, 2001). Descriptions of the best-fitting models for each observer in each biasing condition are presented in Table 10. Consistent with the preceding analyses, the best-fitting models for the neutral conditions allowed preservation of PI, PS, and DS for all observers. For the condition favoring curvature, the models showed a single violation of PS for one observer, and consistent violations of DS on just one dimension for all observers. The same result was obtained for the condition biased against curvature: the best-fitting models for all of the observers contained a violation of DS on just one dimension.

Predicted effects of a violation of DS on capacity

Having established that we were able to induce regular violations of DS with our biasing manipulations in the CID,

we can now inquire as to the effects that such violations might have in the context of the DFP. Consider that the violations of DS that we observed occurred on only one of the two dimensions. Now consider that the cells of the CID that provide the data for observing this violation are the cells in the DFP that are used to estimate capacity (see Fig. 4a) using the AND version of the capacity coefficient

$$C_A(t) = \frac{\ln[F_L(t)] + \ln[F_R(t)]}{\ln[F_{LR}(t)]},$$

where $F_L(t)$, $F_R(t)$ and $F_{LR}(t)$ are, respectively, the cumulative distribution functions for the conditions in which the left, right, and both sides are curved. Finally, consider that we obtained two types of violation of DS, one in favor of curved responses in the curved/curved trials (Fig. 4b), and one in favor of straight responses. From Fig. 4b and c we can see that the RTs in the DFP that will be affected should be those for the straight/curved and curved/curved stimuli. In order to obtain predictions for the

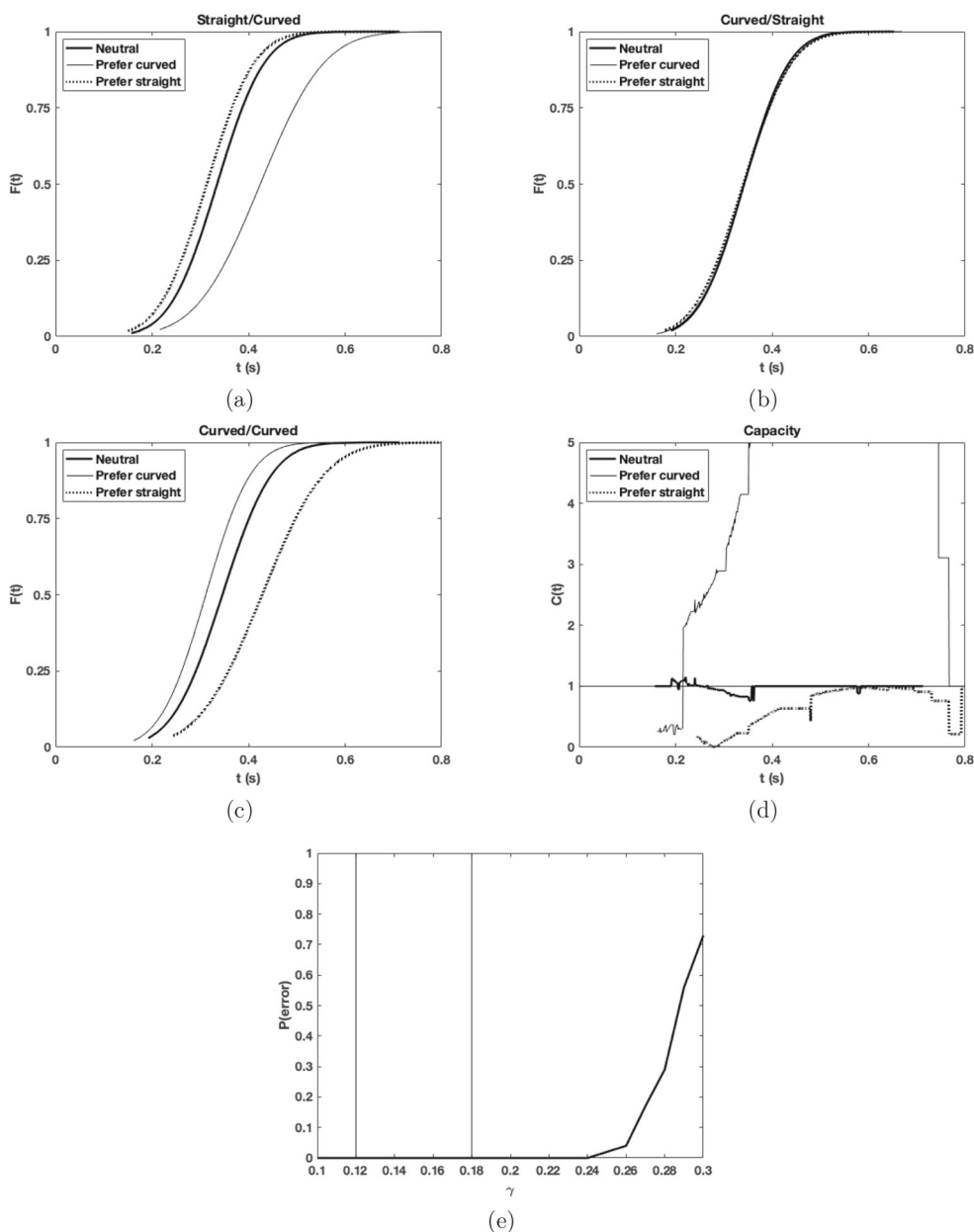


Fig. 5 Simulation results: Cumulative distribution functions (cdf) (a) for the trials involving the straight/curved stimuli (b) for the trials involving the curved/straight stimuli, and (c) for the trials involving the curved/curved stimuli. **d** Predicted effects on the capacity coefficient $C_A(t)$. **e** Predicted error rates as a function of the activation threshold γ ; the pair of vertical lines indicate the range of γ used in the simulations

effects of these violations of DS on capacity, we simulated these conditions using the linear dynamic systems modeling approach that we have used in previous work (Townsend & Wenger, 2004, 2006, 2012). Details of this modeling are presented in the Appendix and the results of the simulations are presented in Fig. 5.

Consistent with our expectations, neither of the shifts in decision bounds predicts an effect on RTs in the curved/straight condition (Fig. 5b). In the case in which the shift in the decision bound is to favor a curved response in the curved/curved condition, we see opposing effects in the

cumulative distribution functions for the straight/curved and curved/curved conditions. For the straight/curved condition, the shift in the decision bound in favor of the curved response for the right side is a shift against the straight response for the right side, which results in a slowing of the RTs for the straight/curved stimuli (Fig. 5a). These are the RTs that contribute to the numerator of the capacity coefficient $C_A(t)$. For the curved/curved condition (Fig. 5c), we obtain a slight speeding-up of RTs due to statistical facilitation (Gumbel, 1958), with these being the denominator of $C_A(t)$. This slowing of one of the

Table 11 Results of the pairwise Kolmogorov–Smirnov tests of stochastic dominance

Obs	Comparison	Neutral	Prefer Curvature	Obs	Comparison	Neutral	Prefer Straight
1	SS vs. SF	2.27 [‡]	2.39 [‡]	2	SS vs. SF	2.18 [†]	2.52 [‡]
	SS vs. FS	1.83 [†]	2.24 [†]		SS vs. FS	1.73 [*]	1.85 [*]
	SS vs. FF	6.28 [‡]	7.09 [‡]		SS vs. FF	8.07 [‡]	8.45 [‡]
	SF vs. FS	0.082	1.07		SF vs. FS	1.40 [*]	1.06
	SF vs. FF	4.31 [‡]	5.83 [‡]		SF vs. FF	7.47 [‡]	8.06 [‡]
	FS vs. FF	4.78 [‡]	6.61 [‡]		FS vs. FF	8.24 [‡]	8.00 [‡]
4	SS vs. SF	1.83 [†]	1.65 [*]	7	SS vs. SF	1.83 [*]	2.22 [‡]
	SS vs. FS	1.71 [†]	1.83 [*]		SS vs. FS	2.64 [‡]	2.29 [‡]
	SS vs. FF	5.65 [‡]	4.22 [‡]		SS vs. FF	7.75 [‡]	8.89 [‡]
	SF vs. FS	0.81	0.70		SF vs. FS	1.34 [*]	1.07
	SF vs. FF	4.78 [‡]	3.69 [‡]		SF vs. FF	7.33 [‡]	9.29 [‡]
	FS vs. FF	4.43 [‡]	3.24 [‡]		FS vs. FF	7.59 [‡]	9.52 [‡]
6	SS vs. SF	2.22 [†]	2.41 [‡]	10	SS vs. SF	2.96 [‡]	3.30 [‡]
	SS vs. FS	1.96 [†]	8.88 [‡]		SS vs. FS	1.93 [*]	1.96 [*]
	SS vs. FF	9.10 [‡]	2.48 [‡]		SS vs. FF	8.38 [‡]	10.13 [‡]
	SF vs. FS	1.02	0.83		SF vs. FS	2.91 [‡]	1.51 [*]
	SF vs. FF	8.57 [‡]	8.31 [‡]		SF vs. FF	7.96 [‡]	9.80 [‡]
	FS vs. FF	8.77 [‡]	8.77 [‡]		FS vs. FF	8.62 [‡]	9.89 [‡]
8	SS vs. SF	2.09 [†]	1.74 [*]				
	SS vs. FS	1.67 ⁺	2.13 [†]				
	SS vs. FF	7.13 [‡]	7.71 [‡]				
	SF vs. FS	0.91	0.84				
	SF vs. FF	5.79 [‡]	6.60 [‡]				
	FS vs. FF	5.71 [‡]	6.12 [‡]				

Note: + = $0.05 \leq p < .10$, * = $p < .05$, † = $p < .01$, ‡ = $p < .001$

single-target distributions and slight speeding-up of the double-target distributions has the net effect of predicting an increase in $C_A(t)$ (Fig. 5d). In the case in which the shift in the decision bound is to favor a straight response in the curved/curved condition, we get opposite effects: a slight speeding-up of the straight/curved RTs and a substantial slowing of the curved/curved RTs, which results in a reduction in $C_A(t)$. Intriguingly, Fig. 5e reveals that in our dynamic stochastic linear systems model, fairly substantial changes in the decision criteria can occur such that processing times are significantly affected without accompanying alterations in accuracy. The outcome can be sizeable effects on $C_A(t)$ absent effects on accuracy. In sum, our simulations predict that a shift in favor of a curved response should result in an increase in capacity, while a shift in favor of a straight response should result in a reduction in capacity.

Double-factorial paradigm

Having established that we were able to induce regular violations of DS with our biasing manipulations in the CID, we can examine observers' performance in the DFP, before and after experiencing the biasing manipulation. In order for inferences to be drawn with respect to architecture and stopping rule, we need to first establish that the distributions of RTs in the double-target condition were ordered consistent with the assumption of selective influence (Townsend & Nozawa, 1995). Results of these tests are presented for all observers in both biasing conditions in Table 11, with the simple result being that proper and reliable orderings were obtained in all cases.

We then examined the interaction contrasts for the double target trials, first at the level of the survivor function of the

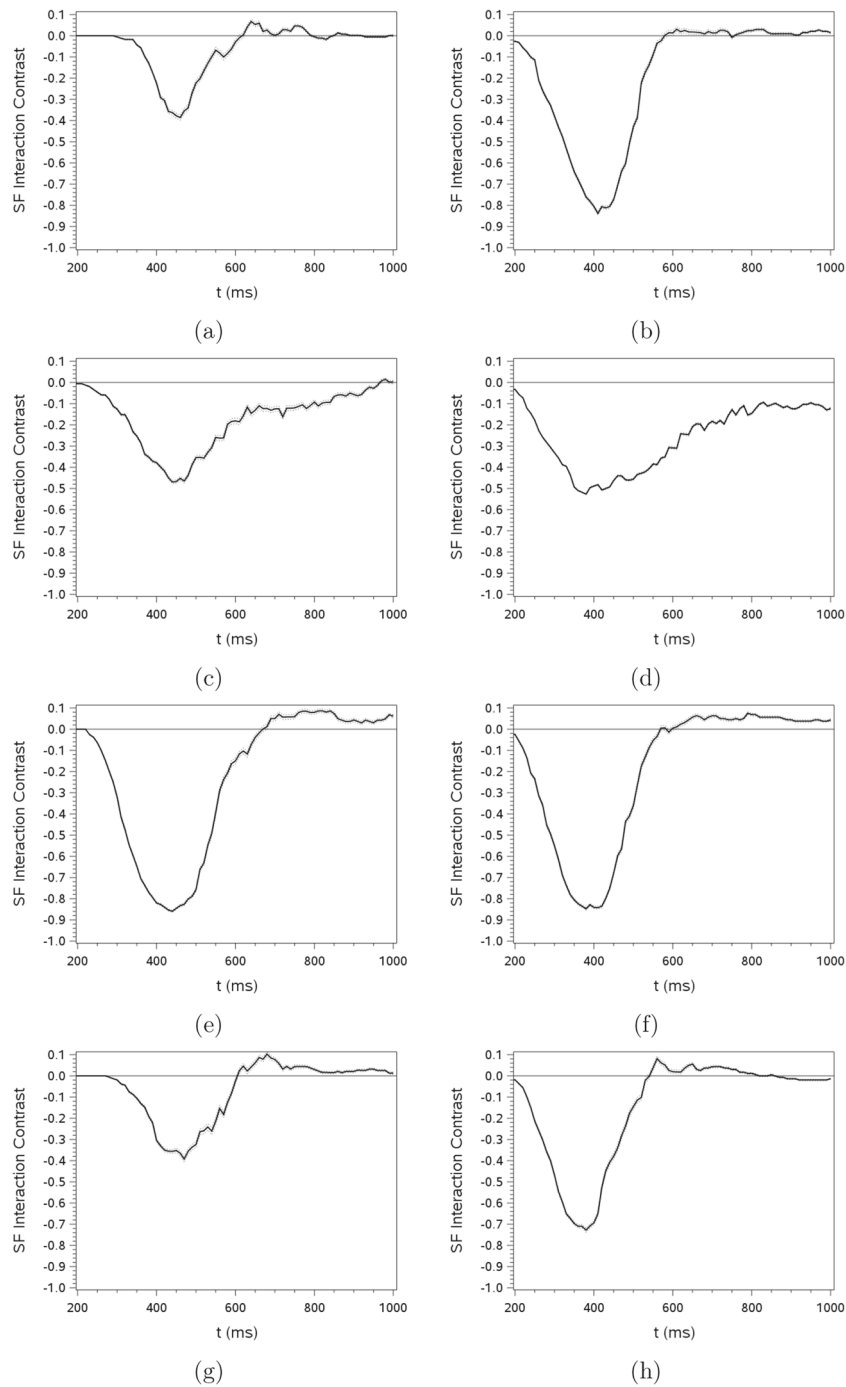


Fig. 6 Survivor function interaction contrasts for the four observers who were switched to a bias in favor of curvature. **a** Obs 1, neutral; **b** obs. 1, prefer curvature; **c** obs. 4, neutral, **d** obs. 4, prefer curvature; **e** obs. 6, neutral; **f** obs. 6, prefer curvature; **g** obs. 8, neutral; **h** obs. 8, prefer curvature

RT distribution. This survivor function interaction contrast (SIC), defined as

$$SIC = [S_{ss}(t) - S_{sf}(t)] - [S_{fs}(t) - S_{ff}(t)]$$

along with the mean interaction contrast (MIC), defined as

$$MIC = (\overline{RT}_{ss} - \overline{RT}_{sf}) - (\overline{RT}_{fs} - \overline{RT}_{ff}),$$

where the subscripts f and s denote the fast and slow conditions, allows for strong inferences regarding processing architecture and stopping rule. The SICs for all observers who were switched from a neutral to bias in favor of curvature are presented in Fig. 6, and the SICs for those who were switched from a neutral to a bias against are presented in Fig. 7. Solid lines in each panel

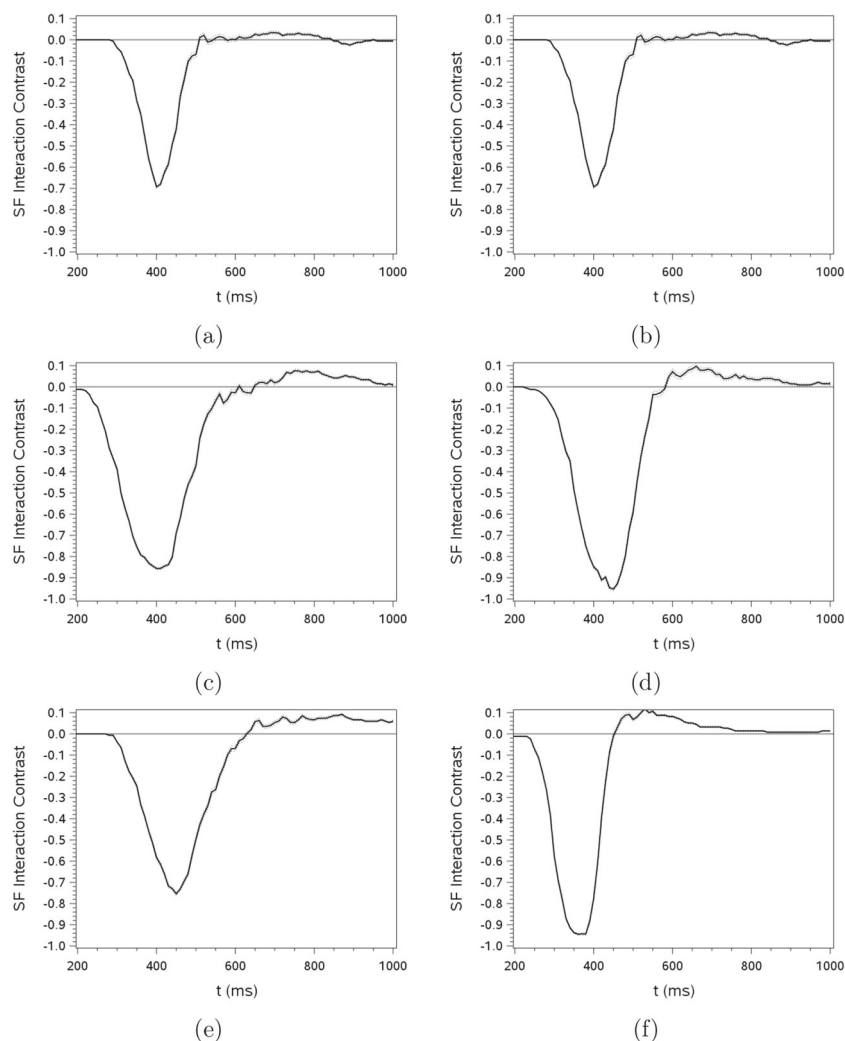


Fig. 7 Survivor function interaction contrasts for the three observers who were switched to a bias against curvature. **a** Obs 2, neutral; **b** obs. 2, prefer straight; **c** obs. 7, neutral; **d** obs. 7, prefer straight; **e** obs. 10, neutral; **f** obs. 10, prefer straight

present the SIC and the dashed lines represent the upper and lower limits of a 95% confidence interval, as estimated by bootstrap.² As can be seen in these figures, the SICs for all observers in both neutral and biased conditions were overwhelmingly negative, from which we infer parallel exhaustive processing of the two sets of lines. No noticeable shifts in the SICs were noted as a function of having experienced the biasing manipulation.

The results of analyzing the data in terms of the main effects and (more importantly) their interaction are presented in Table 12. The interactions for all observers

²For each SIC, 140 observations were drawn with replacement, and the SIC was estimated 1000 times.

in both the neutral and biased conditions were significant and the MICs were all reliably < 0 . Taken together with the SICs, these results unambiguously indicate parallel exhaustive processing in both the neutral and biased conditions, with no differences in terms of the valence of the induced bias. This consistency is almost startling, given the response demands, which allowed for parallel self-terminating processing. It appears that in the presence of this illusion and the varying payoff structures participants opted to engage in exhaustive processing, consistent with notions of configural processing (Townsend & Wenger, 2015). It is quite rare to find pure exhaustive processing where it is possible to obtain perfect accuracy with a minimum time stopping rule.

Table 12 Tests of the interactions at the level of the means

Obs	Bias	Effect	<i>F</i>	<i>MSE</i>	<i>MIC</i>	Bias	Effect	<i>F</i>	<i>MSE</i>	<i>MIC</i>
1	neutral	left curvature (L)	27.07 [‡]	15359		prefer curvature	L	80.48 [‡]	19713	
		right curvature (R)	67.65 [‡]				R	83.12 [‡]		
		L x R	7.27 [†]				L x R	12.26 [‡]		
4	neutral	L	46.62 [‡]	50210		prefer curvature	L	44.60 [‡]	65927	
		R	48.23 [‡]				R	41.74 [‡]		
		L x R	13.42 [‡]				L x R	11.26 [‡]		
6	neutral	L	48.38 [‡]	33184		prefer curvature	L	91.51 [‡]	18047	
		R	58.04 [‡]				R	166.03 [‡]		
		L x R	34.19 [‡]				L x R	36.66 [‡]		
8	neutral	L	55.59 [‡]	18339		prefer curvature	L	175.74 [‡]	11984	
		R	72.28 [‡]				R	128.89 [‡]		
		L x R	4.49 [*]				L x R	49.00 [‡]		
2	neutral	L	13.26 [‡]	9644		prefer straight	L	66.86 [‡]		
		R	16.56 [‡]				R	114.05 [‡]		
		L x R	17.63 [‡]				L x R	13.83 [‡]		
7	neutral	L	185.65 [‡]	18417		prefer straight	L	154.43 [‡]	17581	
		R	175.74 [‡]				R	148.49 [‡]		
		L x R	48.36 [‡]				L x R	38.65 [‡]		
10	neutral	L	71.25 [‡]	18562		prefer straight	L	77.72 [‡]	4202	
		R	212.93 [‡]				R	44.07 [‡]		
		L x R	15.56 [‡]				L x R	83.02 [‡]		

Note: * = $p < .05$, † = $p < .01$, ‡ = $p < .001$

We next examined the capacity coefficients, and plots of all $C(t)$ s are presented for those transferred to a bias in favor of curvature in Fig. 8 and for those transferred to a bias against curvature in Fig. 9. In addition, Figs. 10 and 11 plot the difference between the capacity coefficients in the biased and neutral conditions for the two biasing conditions. We should note that accuracy for all observers was > 94% in all cases, consequently we used the form of the capacity coefficient that is based only on correct trials (Townsend & Nozawa, 1995; Townsend & Wenger, 2004) rather than the form that takes accuracy into account (Townsend & Altieri, 2012). In each panel of Figs. 8 and 9, the solid line represents the value of $C_A(t)$ while the dotted lines plot the upper and lower bounds of the 95% confidence interval, as estimated by bootstrap. For those transferred to the positive bias condition, $C_A(t)$ was reliably > 1 both in the neutral and the positive bias condition, and capacity increased after the transfer to the positive bias condition (see Fig. 10). For those transferred to the negative bias condition, $C_A(t)$ was reliably > 1 in the neutral condition, and decreased to no longer being reliably different from 1 for two observers, and simply decreased for the third (see Fig. 11).

Discussion

In the present study, we sought to determine whether an induced violation of DS would be accompanied by other regular changes in RT-based measures for GRT and in any characteristics of processing in the DFP. We demonstrated in the CID that our manipulations reliably and consistently varied response frequencies in the desired directions and that these were revealed in the analysis of the response frequencies as reliable shifts in c , reliable violations of MRI and tMRI, and with multivariate gaussian model fitting concurring in the inference of violations of DS in the biased conditions. We should emphasize that the evidence from all of these measures was consistent in pointing to violations of DS in the two bias conditions. This was obtained with there being no evidence in either response frequencies or RTs suggestive of violations of PI for any of the observers in any of the conditions. In addition, there was only a single case in which there was evidence to support a violation of PS and, in this case, the change in response frequencies under the bias manipulations was consistent with the direction of the induced bias.

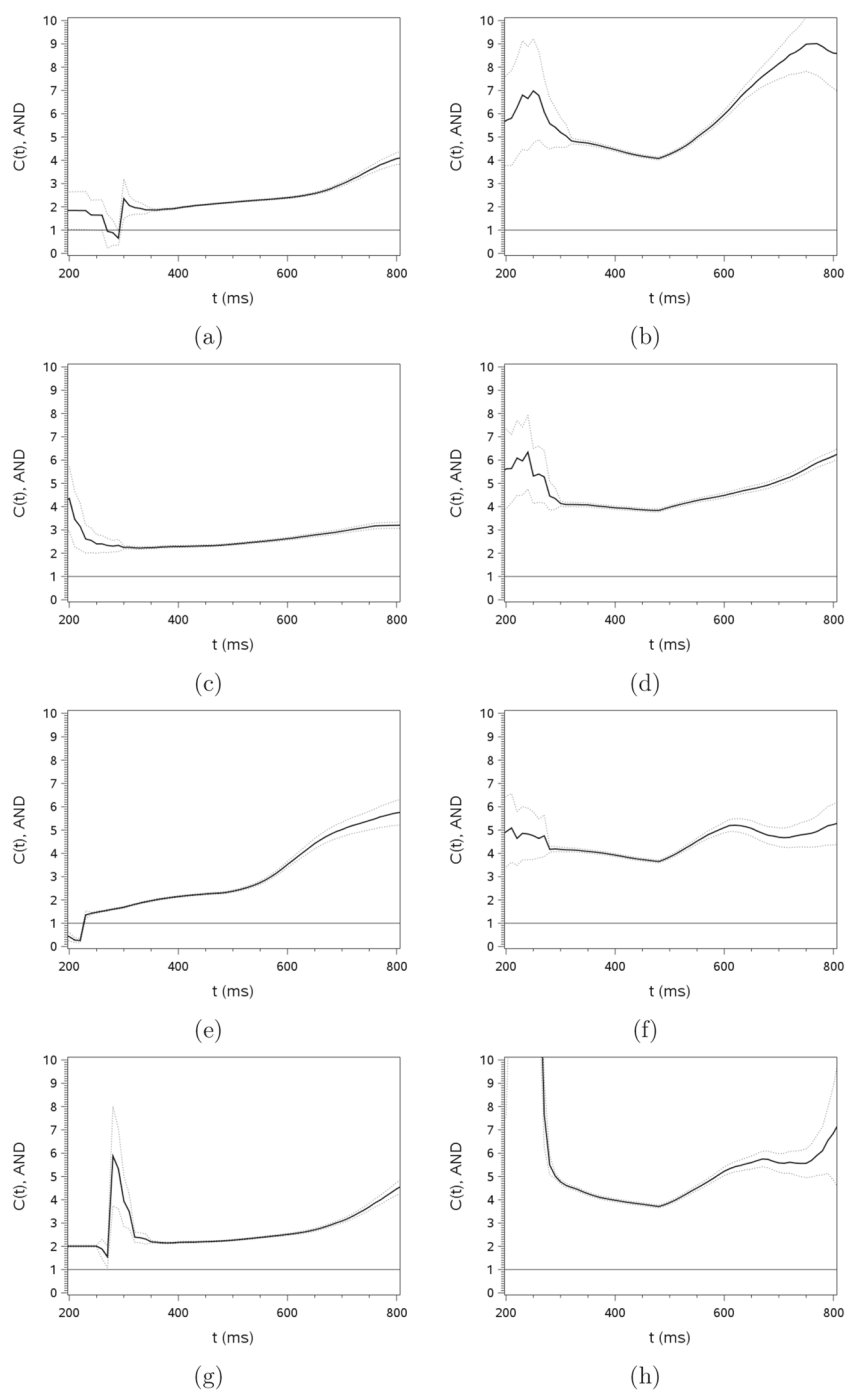


Fig. 8 Capacity coefficients for the four observers who were switched to a bias in favor of curvature: **a** obs. 1, neutral, **b** obs. 1, prefer curvature; **c** obs. 4, neutral; **d** obs. 4, prefer curvature; **e** obs. 6., neutral; **f** obs. 6, prefer curvature; **g** obs. 8, neutral; **h** obs. 8, prefer curvature

We further demonstrated in the DFP that, consistent with our dynamic systems modeling, the induced bias was accompanied by shifts in capacity: inducing a bias in favor of curvature was associated with an increase in capacity, and inducing a bias against curvature was associated with a decrease in capacity. No other changes

in processing characteristics were noted, with all observers in both bias conditions engaging in parallel exhaustive processing, in spite of a response instruction that allowed for self-terminating processing. This relationship between variations in a decisional operator and variations in capacity was first noted in our earlier work on faces and

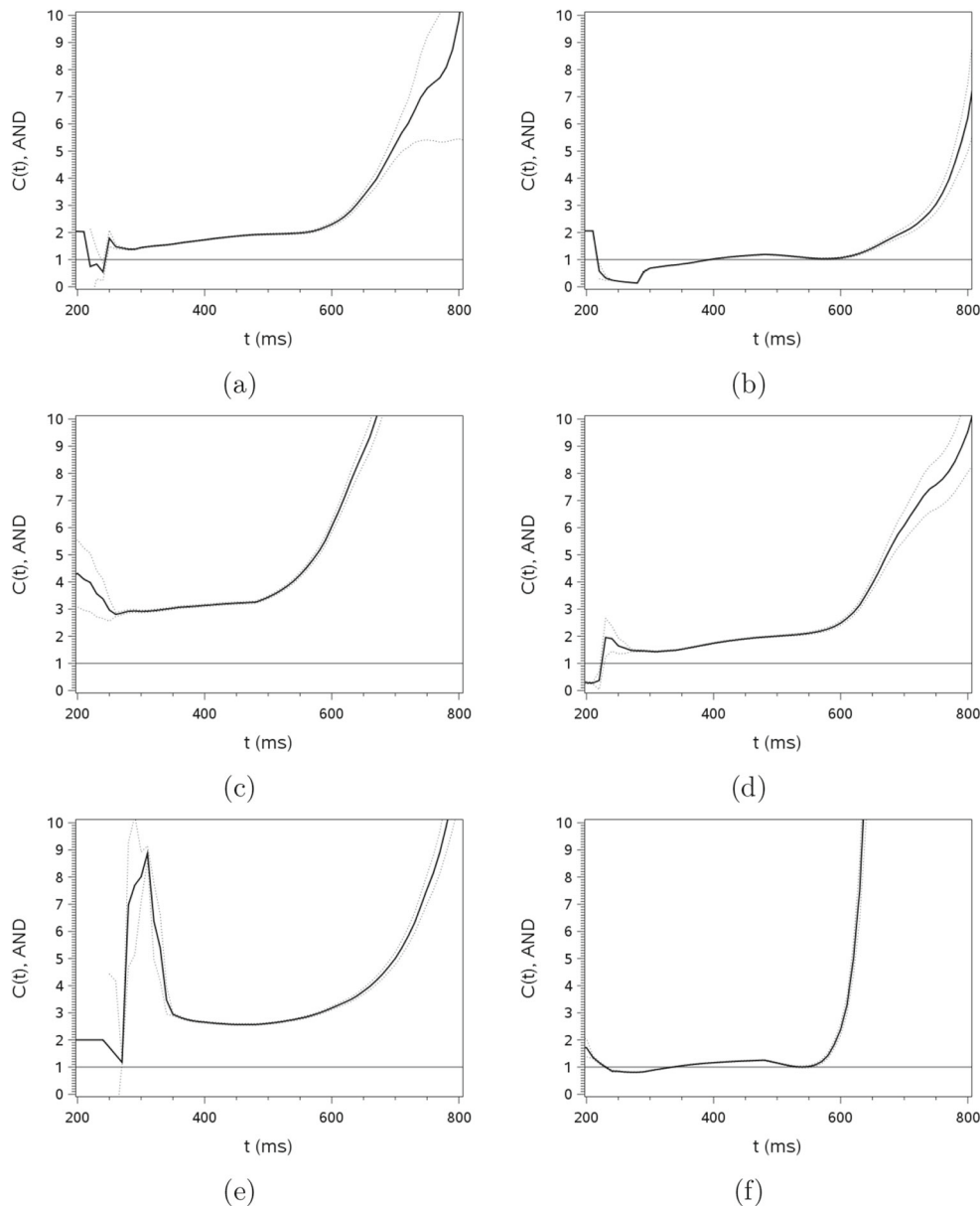


Fig. 9 Capacity coefficients for the four observers who were switched to a bias against curvature: **a** obs. 2, neutral, **b** obs. 2, prefer straight; **c** obs. 7, neutral; **d** obs. 7, prefer straight; **e** obs 10, neutral; **f** obs. 10, prefer straight

words (Wenger & Townsend, 2006), where a model that incorporated changes in a decisional operator best explained the observed changes in capacity.

General discussion

The present results unequivocally do not and are not intended to solve the identifiability issues with the 2×2 version of the CID. What we can claim instead is that induced violations of DS in the CID were regularly associated with changes in capacity in the DFP, and that these two sources of evidence, along with the findings from

our dynamic systems modeling, converge with respect to an inference of a violation of DS.³

It is possible that a transformation such as those discussed by Silbert and Thomas (2013, 2017) could

³Much of the problem, as noted by Silbert and Thomas (2013, 2017), is in the basic 2×2 design. As discussed by Ashby and Wenger (2021), a simple solution is to expand the task to a 3×3 design. In this case, there are enough degrees of freedom in the data to allow a violation of DS to be identified without constraints (e.g., equal variances across all stimulus representations). In addition, the general configuration of the four decision bounds that are needed are such that no linear transformation of the bounds is possible to guarantee that DS holds. Ashby and Wenger (2021) note additional conditions that do allow DS to be identifiable.

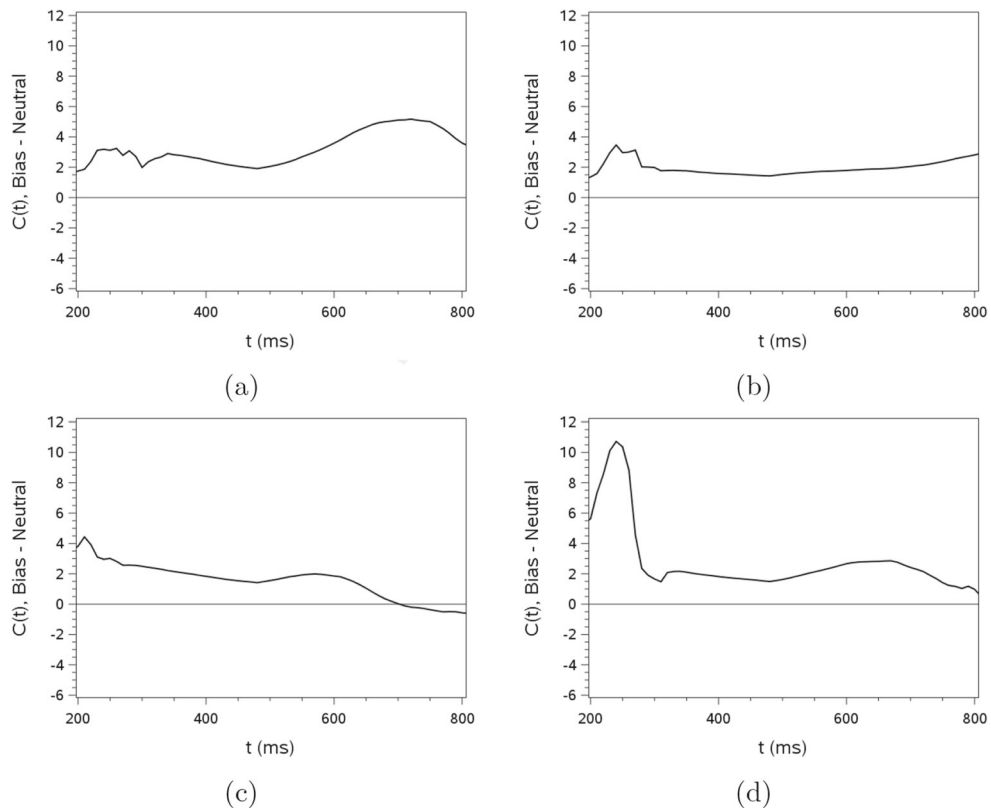


Fig. 10 Difference in $C_A(t)$, bias - neutral, for observers who were switched to a bias in favor of curvature: **a** obs. 1, **b** obs. 4, **c** obs. 6, **d** obs. 8

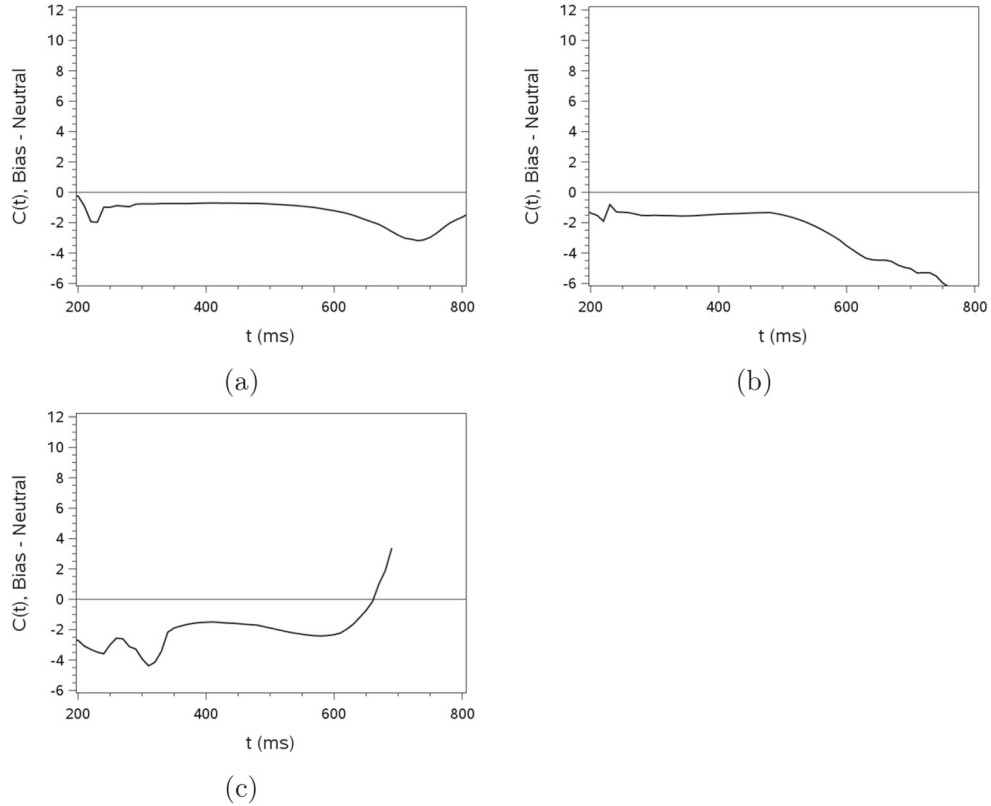


Fig. 11 Difference in $C_A(t)$, bias - neutral, for observers who were switched to a bias against curvature: **a** obs. 2, **b** obs. 7, **c** obs. 10

produce some of the same results. However, it is notable that the several bias conditions lead to quite parsimonious and regular findings in a way very consonant with the experimental manipulations. Thus, we contend that violations of DS more elegantly explain our results than would a violation of either PS or PI. This is important, as it illustrates the need for GRT to be able to consider hypothesized and actual shifts in response criteria as the basis for behavioral regularities. It simply is not sufficient to a priori assume preservation of DS in all cases.

An unexpected but intriguing result from our simulations was that we were able to identify a range of values for the decisional operator (the activation threshold) over which it was possible to see large changes in capacity without any changes in accuracy. This goes against intuition based on classic speed/accuracy tradeoffs (e.g., Doshier, 1979; Wickelgren, 1977) and to our knowledge is the first observation of its kind. Further theoretical and empirical work will be needed to understand the boundary conditions and robustness of this finding.

A violation of DS is a form of integrality that has been suggested as one of the sources for effects that have been interpreted as perceptually holistic (e.g., Wenger & Ingvalson, 2002, 2003). Here we obtained this integrality by manipulating a visual illusion. This phenomenon therefore represents a truly psychological integrality, which is important given that dimensional interactions at the level of decisional operators is distinctly something “inside the head” and not of necessity determined by the physical characteristics of the stimuli.

The present results also speak to the power of combining the measurement approaches of GRT and SFT along with the insights allowed by our linear systems modeling. We previously have shown the potential for supporting strong inferences by combining the two approaches to questions pertaining to perceptual learning (Wenger & Rhoten, 2020). We believe that the current results further reinforce this point. Taking the main analyses all together, we conclude that processing on the two sides of the Hering stimuli were perceptual independent, perceived in parallel with an exhaustive processing rule, in a super capacity fashion and in such a fashion that bias manipulations influenced processing speed without a significant effect on accuracy.

The surprising finding of super capacity while accompanied (at least in the GRT phase of the study) by perceptual independence and the rather startling implementation of a (quite inefficient) exhaustive decision stopping rule are intriguing and merit further exploration. We are in the process of constructing experimental designs which engage SFT and GRT tools over the same sets of trials. This new direction may aid in explaining some of the current puzzles.

In sum, we have shown that it is possible to induce regular violations of DS in the context of a classical illusion,

and that these violations are associated in a regular and interpretable way with changes in capacity. We believe this finding suggests avenues for testing hypotheses regarding varieties of independence and dependence in perception that do not require the strong a priori assumption that DS always holds. In addition, for the most part, illusions have existed more or less as *experimenta demonstranda* (as Boring, 1957, expressed it) for over a century. The current explorations may help lead to more detailed knowledge concerning their information processing mechanisms.

Open Practices Statement None of the data or materials for the experiments reported here is available, and none of the experiments was preregistered.

Appendix: Linear Systems Simulations

To obtain the predictions for the effects of a violation of DS on capacity in the DFP, we used the linear dynamic systems approach that we have used in prior efforts (Townsend & Wenger 2004, 2006, 2012). A schematic representation of the specific model used in the present application is shown in Fig. 12. The model is a system composed of two parallel channels that can be described by system of differential equations:

$$\frac{d}{dt}\mathbf{x}(t) = \mathbf{A}\mathbf{x}(t) + \mathbf{B}\mathbf{u}(t)$$

Here $\mathbf{x}(t)$ is a two-element vector representing the activation in the two channels processing the left and right set of elements in the stimulus, $x_L(t)$ and $x_R(t)$, respectively. The inputs to the system are represented by the two-element vector

$$\mathbf{u}(t) = \begin{bmatrix} u_L + N(0, \sigma, t) \\ u_R + N(0, \sigma, t) \end{bmatrix}$$

where u_L and u_R are constants (positive for curved inputs, negative for straight inputs) to which at each time point a sample of Gaussian noise is added, with those samples being uncorrelated across the channels. The inputs are distributed to the two channels according to the 2×2 matrix \mathbf{B} which we here assume to be

$$\mathbf{B} = \mathbf{I}.$$

The channel rate parameters are given by the elements of the 2×2 matrix

$$\mathbf{A} = \begin{bmatrix} a_{LL} & 0 \\ 0 & a_{RR} \end{bmatrix}$$

with the additional constraint that $a_{LL} = a_{RR}$. Absolute values of the channel activations at each time point were compared against threshold values γ_L and γ_R and the processing times for each channel, T_L, T_R , were taken as the first time for which $|x_i(t)| > \gamma_i, i = L, R$. The response

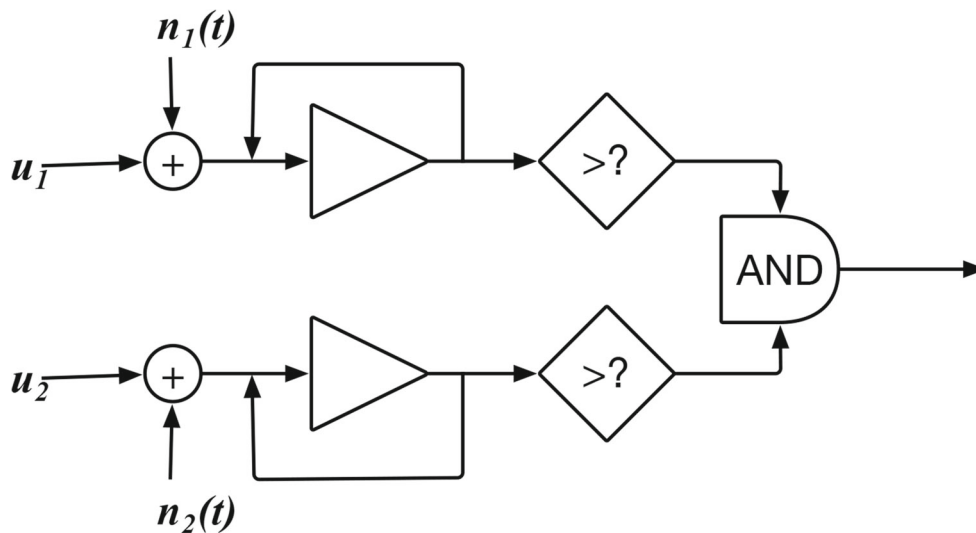


Fig. 12 Schematic representation of the linear dynamic system used to obtain the predictions for capacity

time on each simulated trial was

$$RT = \max[T_L, T_R]$$

and the response choice was determined by the sign of the channel activations associated with the longest processing time, with positive values corresponding to a choice of “curved” and negative values corresponding to a choice of “straight.”

Numeric values for all of the simulation parameters are presented in Table 13. As noted in the text, the critical values for the simulations are the values of the channel criteria, γ_L and γ_R . In the neutral case, $\gamma_L = \gamma_R = 0.15$. In the case in which the preferred response was “curved,” γ_L for the curved/curved stimulus was set to 0.12 and γ_L for the straight/curved stimulus was set to 0.18. In the case in which the preferred response was “straight,” γ_L for the curved/curved stimulus was set to 0.18 and γ_L for the straight/curved stimulus was set to 0.12. For all of these cases, γ_R remained constant at 0.15.

Table 13 Parameters and values for the linear dynamic systems simulations

Parameter	Role	Value
N	Trials per stimulus	500
u_L, u_R	Constant channel inputs	0.75 = curved, -0.75 = straight
σ^2	Power, Gaussian input noise	0.005
a_{LL}, a_{rr}	Channel rate parameters	-3.0
γ_L, γ_R	Channel activation thresholds	0.15, neutral case

References

- Ashby, F. G., & Townsend, J. T. (1986). Varieties of perceptual independence. *Psychological Review*, *93*, 154–179.
- Ashby, F. G., & Wenger, M. J. (2021). Statistical decision theory. In Ashby, F. G., Colonius, H., & Dzhafarov, E. N. (Eds.) *The New Handbook of Mathematical Psychology, Volume 3: Perceptual and Cognitive Processes*: Cambridge.
- Balakrishnan, J. D. (1999). Decision processes in discrimination: Fundamental misrepresentations of signal detection theory. *Journal of Experimental Psychology: Human Perception and Performance*, *25*(5), 1189.
- Boring, E. G. (1957). *History of experimental psychology*. New York: Appleton-Century-Crofts.
- Cornes, K., Donnelly, N., Godwin, H., & Wenger, M. J. (2011). Perceptual and decisional factors affecting the detection of the Thatcher illusion. *Journal of Experimental Psychology: Human Perception and Performance*, *37*, 645–668.
- Doshier, B. A. (1979). Empirical approaches to information processing: Speed-accuracy tradeoff functions or reaction time—a reply. *Acta Psychologica*, *43*, 347–359.
- Dzhafarov, E., & Colonius, H. (1999). Fechnerian metrics in unidimensional and multidimensional stimulus spaces. *Psychonomic Bulletin and Review*, *6*, 239–268.
- Egan, J. P. (1975). *Signal detection theory and roc analysis*. New York: Academic.
- Estes, W. K. (2002). Traps in the route to models of memory and decision. *Psychonomic Bulletin & Review*, *9*(1), 3–25.
- Forster, K. I., & Forster, J. C. (2003). DMDX: A Windows display program with millisecond accuracy. *Behavioral Research Methods, Instruments, and Computers*, *35*, 116–124.
- Garner, W. R., Hake, H. W., & Eriksen, C. W. (1956). Operationism and the concept of perception. *Psychological review*, *63*(3), 149.
- Gourevitch, V., & Galanter, E. (1967). A significance test for one parameter isosensitivity functions. *Psychometrika*, *32*, 25–33.
- Gumbel, E. J. (1958). *Statistics of extremes*. New York: Columbia University Press.
- Hansen, K. H. (1961). Hering’s illusion. *British Journal of Psychology*, *52*(4), 317–321.

- Hering, E. (1861). *Beiträge zur physiologie*. Leipzig: W. Engelmann.
- Link, S. W. (1994). Rediscovering the past: Gustav Fechner and signal detection theory. *Psychological Science*, *5*(6), 335–340.
- Little, D., Altieri, N., Yang, C. T., & Fific, M. (2017). *Systems factorial technology: A theory driven methodology for the identification of perceptual and cognitive mechanisms*. Elsevier Science & Technology Books. Retrieved from <https://books.google.com/books?id=OQICMQAACAAJ>.
- Macmillan, N. A., & Creelman, C. D. (2004). *Detection theory: A user's guide*. Psychology press.
- Murray, D. J., & Link, S. W. (2021). *The Creation of scientific psychology*. Routledge.
- Silbert, N. H., & Thomas, R. D. (2013). Decisional separability, model identification, and statistical inference in the general recognition theory framework. *Psychonomic Bulletin & Review*, *1*–20.
- Silbert, N. H., & Thomas, R. D. (2017). Identifiability and testability in GRT with individual differences. *Journal of Mathematical Psychology*, *77*, 187–196.
- Silbert, N. H., & Hawkins, R. X. D. (2016). A tutorial on General Recognition Theory. *Journal of Mathematical Psychology*, *73*, 94–109. <https://doi.org/10.1016/j.jmp.2016.04.011>
- Thomas, R. D. (2001). Characterizing perceptual interactions in face identification using multidimensional signal detection theory. In Wenger, M. J., & Townsend, J. T. (Eds.) *Computational, geometric, and process perspectives on facial cognition: Contexts and challenges*, (pp. 193–228). Mahwah: Erlbaum.
- Townsend, J. T., & Altieri, N. (2012). An accuracy-response time capacity assessment function that measures performance against standard parallel predictions. *Psychological Review*, *119*(3), 500–516.
- Townsend, J. T., & Ashby, F. G. (1983). *Stochastic modeling of elementary psychological processes*. Cambridge: Cambridge University press.
- Townsend, J. T., Houpt, J. W., & Silbert, N. H. (2012). General recognition theory extended to include response times: Predictions for a class of parallel systems. *Journal of Mathematical Psychology*, *56*(6), 476–494.
- Townsend, J. T., Hu, G. G., & Kadlec, H. (1988). Feature sensitivity, bias, and interdependencies as a function of intensity and payoffs. *Perception & Psychophysics*, *43*, 575–591.
- Townsend, J. T., & Nozawa, G. (1995). On the spatio-temporal properties of elementary perception: An investigation of parallel, serial, and coactive theories. *Journal of Mathematical Psychology*, *39*, 321–359.
- Townsend, J. T., & Wenger, M. J. (2004). A theory of interactive parallel processing: New capacity measures and predictions for a response time inequality series. *Psychological Review*, *111*, 1003–1035.
- Townsend, J. T., & Wenger, M. J. (2015). On the dynamic perceptual characteristics of gestalten: Theory-based methods. In Wagemans, J. (Ed.) *The Oxford handbook of perceptual organization*, (pp. 948–968). Oxford.
- Wenger, M. J., & Ingvalson, E. M. (2002). A decisional component of holistic encoding. *Journal of Experimental Psychology: Learning, Memory, and Cognition*, *28*, 872–892.
- Wenger, M. J., & Ingvalson, E. M. (2003). Preserving informational separability and violating decisional separability in facial perception and recognition. *Journal of Experimental Psychology: Learning, Memory, and Cognition*, *29*, 1106–1118.
- Wenger, M. J., & Rhoten, S. E. (2020). Perceptual learning produces perceptual objects. *Journal of Experimental Psychology: Learning, Memory, and Cognition*, *46*(3), 455–475.
- Wenger, M. J., & Townsend, J. T. (2006). On the costs and benefits of faces and words. *Journal of Experimental Psychology: Human Perception and Performance*, *32*, 755–779.
- Wickelgren, W. A. (1977). Speed-accuracy tradeoff and information processing dynamics. *Acta Psychologica*, *41*, 67–85.
- Wixted, J. T. (2020). The forgotten history of signal detection theory. *Journal of experimental psychology: learning, memory, and cognition*, *46*(2), 201.

Publisher's note Springer Nature remains neutral with regard to jurisdictional claims in published maps and institutional affiliations.